Binding of Similarly Charged Plates with Counterions Only

André G. Moreira and Roland R. Netz
Max Planck Institute of Colloids and Interfaces, 14424 Potsdam, Germany
(Received 20 September 2000; published 26 July 2001)

Similarly and highly charged plates in the presence of multivalent counterions attract each other and form electrostatically bound states. Using Monte-Carlo simulations, we obtain the interplate pressure in the global parameter space. The equilibrium plate separation, where the pressure changes from attractive to repulsive, exhibits a novel unbinding transition. A systematic and asymptotically exact strong-coupling field theory yields the bound state from a competition between counterion entropy and electrostatic attraction, in agreement with simple scaling arguments and simulations.

DOI: 10.1103/PhysRevLett.87.078301 PACS numbers: 82.70.–y, 82.45.–h, 87.16.Dg

Experimentally, it has been known for a long time that highly charged planar surfaces attract each other in the presence of multivalent counterions, inducing bound states. This electrostatic attraction restricts the swelling of calcium clay particles [1], leads to much reduced water uptake of charged lamellar membrane systems [2], and has also been observed with the surface force apparatus [3]. Monte-Carlo (MC) simulations confirmed that for a given surface charge density there exists a threshold counterion valence above which attraction can be observed over some range of plate separations [4].

Theoretically, these observations came as a surprise, since the mean-field or Poisson-Boltzmann (PB) theory predicts only repulsive forces between similarly charged objects [5]. This contradiction resulted in an immense theoretical activity, which aimed at understanding the simplified model of two uniformly and similarly charged planar surfaces interacting across a gap of width d filled with pointlike counterions only. Clearly, reality is much more complicated due to additional interactions and effects, but even this model, which we consider in this paper, is quite challenging. A number of approaches were proposed which incorporate counterion correlations that are neglected within PB. The first were integral-equation theories [6], perturbative expansions around the PB theory [7,8], and local density-functional theory [9], which compare well with simulation results and exhibit attraction. If the two plates are far apart from each other, the counterion clouds can be viewed as condensed on the plates, and the resulting simplified model can be solved within a Gaussian [10] or harmonic-plasmon approximation [11]. These approaches either involve numerics and do not provide much physical insight, or they are valid for asymptotically large plate separations.

In this paper, we focus on the mechanism for electrostatic attraction between similarly charged plates and, in particular, on the bound state, which occurs for finite plate separations. To do this, we introduce a novel field theory, asymptotically exact in the strong-coupling (SC) limit (equivalent to low temperatures, large plate-charge density σ, and large counterion valence q), which corresponds to a systematic virial (low-density) expansion. The SC theory is valid in the limit when PB breaks down and naturally yields electrostatic attraction between similarly charged plates. To check these theoretical results, we have performed extensive MC simulations in the complete parameter space. In the SC limit, we obtain quantitative agreement of MC density and pressure profiles with our SC theory, whereas PB theory describes the numerical data well in the opposite limit of weak coupling.

The leading term of our SC theory is the first virial term and thus corresponds to the partition function of a single counterion sandwiched between two charged plates, which we now explicitly evaluate, thereby providing some physical insight into the mechanism for electrostatic attraction. That this simple calculation in fact is exact in the SC limit will be demonstrated below in a formal field-theoretic calculation and by comparison with MC results. Denoting the distance between the counterion and the plates (of area A) as x and $d - x$, respectively, we obtain for the electrostatic interaction between the ion and the plates (note that all energies and forces are given in units of k_BT) for $d \ll \sqrt{A}$ the results $W_1 = 2\pi\ell_B q\sigma x$ and $W_2 = 2\pi\ell_B q\sigma(d - x)$, respectively, as follows from the potential at an infinite charged wall and omitting constant terms. The Bjerrum length $\ell_B = e^2/4\pi\varepsilon k_BT$ is the distance at which two unit charges interact with k_BT. The sum of the two interactions is $W_{1+2} = W_1 + W_2 = 2\pi\ell_B q\sigma d$ which shows that (i) no pressure is acting on the counterion since the forces exerted by the two plates exactly cancel, and (ii) that the counterion mediates an effective attraction between the two plates. The interaction between the two plates is proportional to the total charge on one plate, $A\sigma$, and for $d \ll \sqrt{A}$ given by $W_{12} = -2\pi A\ell_B\sigma^2 d$. Since the system is electroneutral, $q = 2A\sigma$, the total energy is $W = W_{12} + W_1 + W_2 = 2\pi A\ell_B\sigma^2 d$, leading to an electrostatic pressure $P_{\rm el} = -\partial(W/A)/\partial d = -2\pi\ell_B\sigma^2$ per unit area. *The two plates attract each other.* The entropic pressure due to counterion confinement is $P_{\rm en} = 1/Ad = 2\sigma/qd$. The equilibrium plate separation is characterized by zero total pressure, $P_{\rm tot} = P_{\rm el} + P_{\rm en} = 0$, leading to an equilibrium plate separation $d^* = 1/\pi\ell_B q\sigma$. In fact, this simple

 0031-9007/01/87(7)/078301(4)$15.00

one-particle derivation for the attraction between charged plates is conceptually simpler than the PB result of repulsion, because the latter case involves many-body effects. Surprisingly, the results for $P_{\rm tot}$ and d^* become exact in the SC limit, as we will demonstrate in the following.

To proceed with our systematic field theory, consider the partition function for N counterions confined between two parallel plates at distance d:

$$\mathcal{Z}_N = \frac{1}{N!}\prod_{j=1}^{N}\int d\mathbf{r}_j\,\theta(z_j)\theta(d-z_j)\mathrm{e}^{-\mathcal{H}}, \qquad (1)$$

where the Heaviside function is defined by $\theta(z)=1$ for $z>0$ and zero otherwise. Introducing the counterion density operator $\hat\rho(\mathbf{r})=\sum_{j=1}^{N}\delta(\mathbf{r}-\mathbf{r}_j)$, the Hamiltonian can be written in units of k_BT as

$$\begin{aligned}\mathcal{H} = \frac{\ell_B}{2}\int d\mathbf{r}\,d\mathbf{r}'[q\hat\rho(\mathbf{r})-\sigma\delta(z)-\sigma\delta(d-z)]\\ \times v(\mathbf{r}-\mathbf{r}')[q\hat\rho(\mathbf{r}')-\sigma\delta(z')-\sigma\delta(d-z')]\\ -\int d\mathbf{r}\,\hat\rho(\mathbf{r})h(\mathbf{r}),\end{aligned} \qquad (2)$$

where $v(\mathbf{r})=1/r$ is the Coulomb interaction, and the field h has been added to calculate density distributions later on. Rescaling all lengths by the Gouy-Chapman length $\mu = 1/2\pi\ell_B q\sigma$ (which is the distance at which a counterion and a charged wall interact with k_BT) according to $\mathbf{r}=\mu\tilde{\mathbf{r}}$ and $d=\mu\tilde d$, the Hamiltonian becomes

$$\begin{aligned}\mathcal{H} = \frac{1}{8\pi^2\Xi}\int d\tilde{\mathbf{r}}\,d\tilde{\mathbf{r}}'[2\pi\Xi\hat\rho(\tilde{\mathbf{r}})-\delta(\tilde z)-\delta(\tilde d-\tilde z)]\\ \times v(\tilde{\mathbf{r}}-\tilde{\mathbf{r}}')[2\pi\Xi\hat\rho(\tilde{\mathbf{r}}')-\delta(\tilde z')-\delta(\tilde d-\tilde z')]\\ -\int d\tilde{\mathbf{r}}\,\hat\rho(\tilde{\mathbf{r}})h(\tilde{\mathbf{r}}),\end{aligned} \qquad (3)$$

and thus depends only on the coupling parameter $\Xi = 2\pi q^3\ell_B^2\sigma$. At this point, we employ a Hubbard-Stratonovitch transformation, similar to previous implementations of a field theory for charged systems [12], followed by a Legendre transformation to the grand-canonical ensemble, $\mathcal{Q}=\sum_N\lambda^N\mathcal{Z}_N$, introducing the fugacity λ. The inverse Coulomb operator follows from Poisson's law as $v^{-1}(\mathbf{r}) = -\nabla^2\delta(\mathbf{r})/4\pi$, which leads to

$$\begin{aligned}\mathcal{Q} = \int\frac{\mathcal{D}\phi}{\mathcal{Z}_v}\exp\Big\{-\frac{1}{8\pi\Xi}\int d\tilde{\mathbf{r}}\{[\nabla\phi(\tilde{\mathbf{r}})]^2-4\imath\delta(\tilde z)\phi(\tilde{\mathbf{r}})\\ -4\imath\delta(\tilde d-\tilde z)\phi(\tilde{\mathbf{r}})\\ -4\Lambda\theta(\tilde z)\theta(\tilde d-\tilde z)\mathrm{e}^{h(\tilde{\mathbf{r}})-\imath\phi(\tilde{\mathbf{r}})}\}\Big\},\end{aligned} \qquad (4)$$

where we introduced the notation $\mathcal{Z}_v=\sqrt{\det v}$ and the rescaled fugacity Λ is defined by $\Lambda = 2\pi\lambda\mu^3\Xi = \lambda/(2\pi\sigma^2\ell_B)$. The field ϕ is the fluctuating electrostatic potential [12]. The expectation value of the counterion density, $\rho(\tilde{\mathbf{r}})$, follows by taking a functional derivative with respect to the generating field h, $\rho(\tilde{\mathbf{r}}) = \delta\ln\mathcal{Q}/\delta h(\tilde{\mathbf{r}})\mu^3$, giving rise to the rescaled density,

$$\tilde\rho(\tilde{\mathbf{r}}) = \frac{\rho(\tilde{\mathbf{r}})}{2\pi\ell_B\sigma^2} = \Lambda\langle\mathrm{e}^{-\imath\phi(\tilde z)}\rangle. \qquad (5)$$

The normalization condition for the counterion distribution, $\mu\int d\tilde z\,\rho(\tilde z)=2\sigma/q$, which follows from the definition of the grand-canonical partition function, leads to

$$\Lambda\int_0^{\tilde d}d\tilde z\langle\mathrm{e}^{-\imath\phi(\tilde z)}\rangle = 2, \qquad (6)$$

and thus fixes the value of Λ. Let us first repeat the saddle-point analysis, which, because of the structure of the action in Eq. (4), should be valid for $\Xi\ll 1$ [12]. The saddle-point equation reads $\partial^2\phi(\tilde z)/\partial\tilde z^2 = 2\imath\Lambda\mathrm{e}^{-\imath\phi(\tilde z)}$, with the solution $\imath\phi(\tilde z) = 2\ln\cos(\Lambda^{1/2}[\tilde z-\tilde d/2])$. The normalization condition Eq. (6) leads to the equation $\Lambda^{1/2}\tan[\tilde d\Lambda^{1/2}/2]=1$, which is solved by $\Lambda\simeq 2/\tilde d - 1/3$ for $\tilde d\ll 1$ and $\Lambda\simeq\pi^2/\tilde d^2$ for $\tilde d\gg 1$. From Eq. (5), the leading term of $\tilde\rho$ is given by the well-known PB result:

$$\tilde\rho(\tilde z) = 1/\cos^2(\Lambda^{1/2}[\tilde z-\tilde d/2]) + \mathcal{O}(\Xi), \qquad (7)$$

with corrections proportional to the coupling constant Ξ [12]. Let us now consider the opposite limit, when the coupling constant Ξ is large and the saddle-point approximation breaks down. Since the fugacity term is bounded, as evidenced by Eq. (6), one can expand the partition function (and also all expectation values) in powers of Λ/Ξ (which is equivalent to a virial expansion). For the expectation value determining the density via Eq. (5), the leading two orders in the virial expansion are

$$\langle\mathrm{e}^{-\imath\phi(\tilde z)}\rangle = \mathrm{e}^{-\Xi v(0)/2} + \frac{\Lambda\mathrm{e}^{-\Xi v(0)}}{2\pi\Xi}\int d\mathbf{r}(\mathrm{e}^{-\Xi v(\mathbf{r}-\tilde{\mathbf{r}})}-1).$$

The normalization condition Eq. (6) can then be solved by an expansion of the fugacity Λ in inverse powers of the coupling constant, $\Lambda=\Lambda_0+\Lambda_1/\Xi+\ldots$, and the leading two terms of the density distribution are

$$\tilde\rho(\tilde z) = \frac{2}{\tilde d} + \frac{2}{\tilde d\Xi}[(\tilde z-\tilde d/2)^2-\tilde d^2/12]. \qquad (8)$$

The leading term, $\tilde\rho_0=2/\tilde d$, is the first virial contribution, which originates from the one-particle partition function, and therefore coincides with the scaling result obtained in the beginning. The second leading term gives a contribution of maximal magnitude $\tilde d/3\Xi$ and therefore dominates the leading term for $\tilde d/\Xi^{1/2} = d/a > 1$, where the mean lateral distance between ions, a, is defined by $2\sigma/q = 1/(\pi a^2)$. This shows that the virial expansion, and, in particular, the SC result, should be valid as long as the plate separation d is smaller than the lateral distance between ions a, or, in rescaled units, for $\tilde d<\Xi^{1/2}$. In Fig. 1a we show density profiles obtained from MC simulations [13] for small coupling parameter $\Xi=0.5$ for various plate distances, which are well described by the PB profiles [Eq. (7)] shown as solid lines. Figure 1b shows that for $\Xi=100$ PB (solid lines) is inadequate [14]. For $\tilde d=1.5$ (open diamonds) we have $d/a=0.15$, and the leading

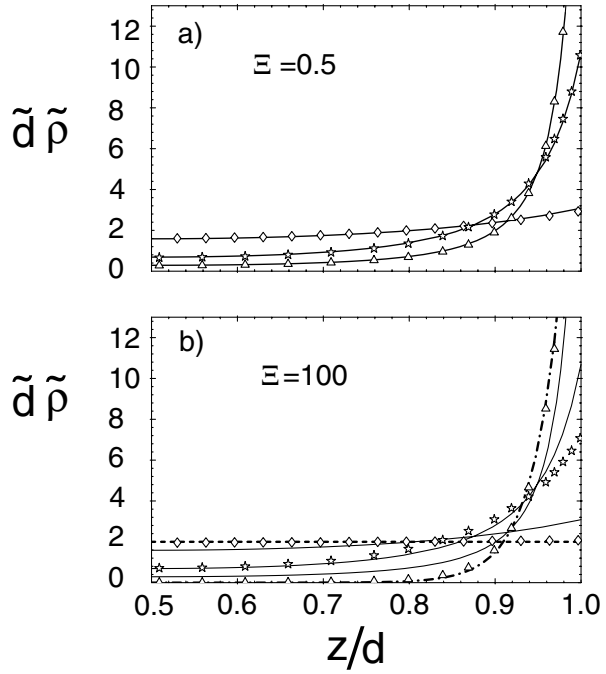

FIG. 1. MC results for the rescaled counterion density $\tilde{d}\tilde{\rho}$ as a function of the rescaled distance from the wall z/d in the (a) PB limit for $\Xi = 0.5$ and in the (b) SC limit for $\Xi = 100$ for various plate separations $\tilde{d} = d/\mu = 1.5$ (open diamonds), $\tilde{d} = 10$ (open stars), and $\tilde{d} = 30$ (open triangles). In (a) MC results agree well with the corresponding PB predictions [Eq. (7), solid lines], whereas in (b) results for $\tilde{d} = 1.5$ agree with the SC prediction $\tilde{\rho} = 2/\tilde{d}$ (dashed line) and for $\tilde{d} = 30$ with a double-exponential curve (dot-dashed line, see text).

term of Eq. (8) is indeed accurate. For $\tilde{d} = 10$ (open stars) we find $d/a = 1$; the density profile is neither described by Eq. (8) nor Eq. (7). Finally, for $\tilde{d} = 30$ (open triangles) we find $d/a = 3$; the two layers are decoupled and the density profile is described by a double-exponential $\tilde{\rho}(\tilde{z}) = (e^{-\tilde{z}} + e^{\tilde{z}-\tilde{d}})/(1 - e^{-\tilde{d}})$ (dot-dashed line), which is the superposition of the density profiles of two isolated charged surfaces in the SC limit [15]. The crossover from PB to SC is demonstrated in Fig. 2, where we plot density profiles for fixed separation $\tilde{d} = 2$ for various coupling parameters Ξ.

Using the contact value theorem, the pressure P between the two plates, which follows from the partition function via $P = \partial \ln \mathcal{Q}_\lambda / A\mu\partial\tilde{d}$, is related to the counterion density at a plate, $\tilde{\rho}(\tilde{d})$, by [4,12]

$$\tilde{P} = P/(2\pi\ell_B\sigma^2) = \tilde{\rho}(\tilde{d}) - 1. \qquad (9)$$

Numerically, the contact ion density $\tilde{\rho}(\tilde{d})$ is obtained from the density profiles by extrapolation. In Fig. 3 we show numerical pressure data for selected values of Ξ. Attraction (negative pressure) is obtained for $\Xi > \Xi^* \approx 12$ and intermediate distances only, as evidenced by the inset where the pressure profile for $\Xi = 17$ is shown. The numerical pressure for $\Xi = 0.5$ (open diamonds) agrees well with the PB prediction (thick solid line), which from

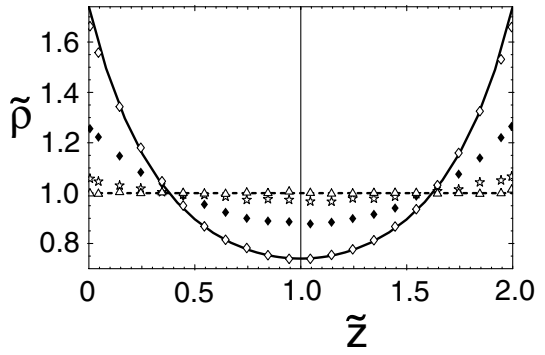

FIG. 2. MC results for rescaled counterion density profiles $\tilde{\rho} = \rho/2\pi\ell_B\sigma^2$ for fixed plate separation $\tilde{d} = d/\mu = 2$ as a function of the rescaled distance $\tilde{z} = z/\mu$ from one wall. Symbols correspond to coupling parameters $\Xi = 0.5$ (open diamonds), $\Xi = 10$ (filled diamonds), $\Xi = 100$ (open stars), and $\Xi = 10^5$ (open triangles), exhibiting clearly the crossover from the PB prediction [solid line, Eq. (7)] to the SC prediction $\tilde{\rho} = 2/\tilde{d}$ [broken line, Eq. (8)].

Eqs. (9) and (7) is given by $\tilde{P} = \Lambda$ with Λ determined by $\Lambda^{1/2}\tan[\tilde{d}\Lambda^{1/2}/2] = 1$. The SC prediction for $\tilde{P}$ is obtained by combining the leading term of Eqs. (8) and (9), yielding $\tilde{P} = 2/\tilde{d} - 1$, from which the equilibrium separation, determined by $\tilde{P} = 0$, follows as $\tilde{d}^* = 2$. Incidentally, this is exactly the scaling prediction for the pressure derived in the beginning of this paper. The small distance range of most data and the complete pressure data for $\Xi = 10^5$ (open triangles) are well described by the SC prediction (broken line), demonstrating again that the SC result is valid for $\tilde{d} < \Xi^{1/2}$.

Finally, combining all pressure data, we obtain the global phase diagram shown in Fig. 4, featuring attractive (negative) interplate pressure at intermediate distances and above a threshold coupling of $\Xi^* \approx 12$. In the limit of large Ξ, the phase boundary saturates at $\tilde{d}^* = 2$, in agreement with our scaling argument and the leading SC term.

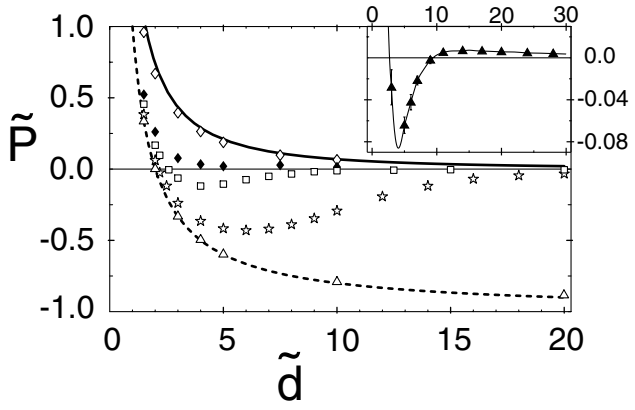

FIG. 3. MC results for the rescaled pressure $\tilde{P}$ as a function of the plate separation $\tilde{d}$ for the same parameter values as in Fig. 2 (and $\Xi = 17$ and 20, filled triangles and open squares, respectively), compared with the PB prediction $\tilde{P} = \Lambda$ (thick solid line) and the SC prediction $\tilde{P} = 2/\tilde{d} - 1$ (broken line).

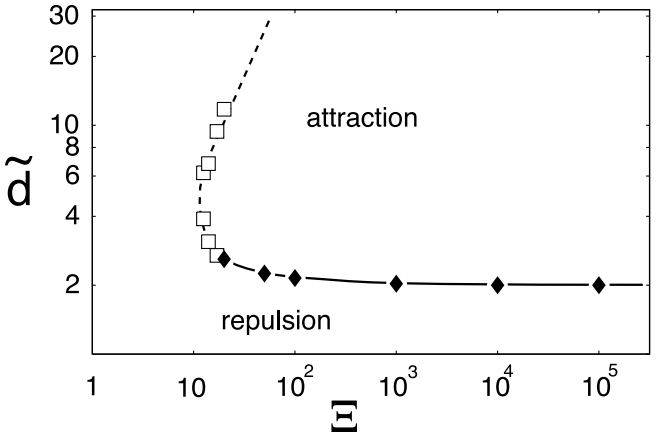

FIG. 4. MC phase diagram showing regions of attractive and repulsive pressure as a function of plate separation $\tilde{d}$ and coupling strength Ξ. Attraction occurs only for intermediate distances and $\Xi > \Xi^* \approx 12$. The equilibrium plate separation (determined by minimization of the free energy, solid line and filled symbols) exhibits a discontinuous unbinding to infinity at $\Xi^{**} \approx 17$ and saturates at $\tilde{d}^* = 2$ for $\Xi \to \infty$.

For large separation reentrant repulsion is observed. The equilibrium plate separation (denoted by filled symbols and a solid line) is determined by a Maxwell construction on the pressure profile, or, equivalently, by minimization of the free energy (which numerically is determined by integrating the pressure). As Ξ decreases from large values, this equilibrium separation grows and shows a discontinuous jump to infinity at $\Xi^{**} \approx 17$ (the corresponding pressure profile is shown in the inset of Fig. 3). For $\Xi < \Xi^{**}$, the lower branch of the broken line (open symbols) corresponds to a local, metastable free-energy minimum while the upper one corresponds to a free-energy maximum. This constitutes a novel unbinding transition, which experimentally is observable with charged lamellar or clay systems by raising the temperature. The reentrant transition from attraction to repulsion at large separations, the upper branch of the broken curve, is expected to scale as $\tilde{d} \sim \Xi$ (plus logarithmic corrections) [7,8], as denoted by the straight broken line and in agreement with the MC data.

The range of validity of our novel SC theory is $\tilde{d} < \sqrt{\Xi}$ which includes most of the equilibrium-plate-separation line in Fig. 4. It follows that the bound state is (i) well characterized by our SC theory (as demonstrated by the fact that the equilibrium plate separation is for the most part close to $\tilde{d}^* = 2$) and (ii) the counterion distribution is indeed two dimensional [16,17], $d < a$, though Wigner crystallization (which occurs at $\Xi \simeq 15\,600$ in the limit $\tilde{d} \to 0$) is not required to find attraction. Correlations between counterions, except the lateral exclusion correlation which keeps ions apart, are unimportant in the bound state for large Ξ, but of course play an important role for intermediate values of Ξ. The range of validity of PB is $\tilde{d} > \Xi \ln\Xi$ for $\Xi > 1$ and $\tilde{d} > 1$ for $\Xi < 1$, as follows by comparison of the PB and one-loop-correction pressures [7,8]. Between the PB and SC ranges of validity is therefore only a small region where none of these asymptotic theories is valid.

Discussions with B. Jönsson and H. Orland are gratefully acknowledged. A. G. M. acknowledges financial support from FCT Praxis XXI (Portugal) and DFG Schwerpunkt Polyelektrolyte (Germany).

[1] R. Kjellander, S. Marcelja, and J. P. Quirk, J. Colloid Interface Sci. **126**, 194 (1988).
[2] H. Wennerström, A. Khan, and B. Lindman, Adv. Colloid Interface Sci. **34**, 433 (1991).
[3] P. Kékicheff, S. Marčelja, T. J. Senden, and V. E. Shubin, J. Chem. Phys. **99**, 6098 (1993).
[4] L. Guldbrand, B. Jönsson, H. Wennerström, and P. Linse, J. Chem. Phys. **80**, 2221 (1984).
[5] D. Andelman, in *Handbook of Biological Physics,* edited by R. Lipowsky and E. Sackmann (Elsevier, New York, 1995), Vol. 1.
[6] R. Kjellander and S. Marčelja, Chem. Phys. Lett. **112**, 49 (1984); J. Phys. Chem. **90**, 1230 (1986).
[7] P. Attard, D. J. Mitchell, and B. W. Ninham, J. Chem. Phys. **88**, 4987 (1988).
[8] R. Podgornik, J. Phys. A **23**, 275 (1990).
[9] M. J. Stevens and M. O. Robbins, Europhys. Lett. **12**, 81 (1990).
[10] P. A. Pincus and S. A. Safran, Europhys. Lett. **42**, 103 (1998).
[11] A. W. C. Lau, D. Levine, and P. Pincus, Phys. Rev. Lett. **84**, 4116 (2000).
[12] R. R. Netz and H. Orland, Europhys. Lett. **45**, 726 (1999); Eur. Phys. J. E **1**, 67 (2000); **1**, 203 (2000).
[13] Simulations are typically performed for 10^6 MC steps with 100 to 150 counterions, in which case finite-size effects are negligible. Periodic boundaries are implemented as described in J. Lekner, Physica (Amsterdam) **176A**, 524 (1991); R. Sperb, Mol. Simul. **20**, 179 (1998).
[14] Experimentally, a coupling parameter $\Xi = 100$, which is quite close to the SC limit (see Fig. 4), is reached with divalent/trivalent ions for surface charge densities $\sigma \approx 3.6\ \mathrm{nm}^{-2}$ and $\sigma \approx 1\ \mathrm{nm}^{-2}$, which are feasible values for compressed charged monolayers.
[15] A. G. Moreira and R. R. Netz, Europhys. Lett. **52**, 705 (2000).
[16] I. Rouzina and V. A. Bloomfield, J. Phys. Chem. **100**, 9977 (1996).
[17] B. Shklovskii, Phys. Rev. E **60**, 5802 (1999).